



# Highly efficient blue organic light-emitting devices based on an exciplex host with thermally activated delayed fluorescence

DONG HYUN PARK,<sup>1</sup> DAE HUN KIM,<sup>2</sup> AND TAE WHAN KIM<sup>1,2,\*</sup>

<sup>1</sup>Department of Information Display Engineering, Hanyang University, Seoul 133-791, South Korea

<sup>2</sup>Department of Electronics and Computer Engineering, Hanyang University, Seoul 133-791, South Korea

\* [twk@hanyang.ac.kr](mailto:twk@hanyang.ac.kr)

**Abstract:** Thermally activated delayed fluorescence (TADF) resulting from the harvesting of triplet excitons has currently emerged as an excellent candidate for enhancing the efficiency of organic light-emitting devices (OLEDs). Highly efficient blue OLEDs based on an exciplex host with carbazole/thioxanthene-S, S-dioxide (EBCz-ThX) and 2-phenyl-bis-4, 6-(3, 5-di-4-pyridylphenyl) pyrimidine (B4PYPPM) acting as a blue TADF emitter were fabricated. The maximum values of the current and the power efficiency for the blue OLEDs with an EBCz-ThX:B4PYPPM exciplex host were 22.46 cd/A and 28.23 lm/W, respectively. The power efficiency of blue OLEDs with an exciplex host was much higher than that of conventional blue OLEDs. The efficiency enhancement of the blue OLEDs based on an exciplex system with a TADF emitter was attributed to the efficient up-conversion of the triplet excitons in the EBCz-thx:B4PYPPM and to the efficient energy transfer from the exciplex host to the blue TADF emitter.

© 2018 Optical Society of America under the terms of the [OSA Open Access Publishing Agreement](#)

## 1. Introduction

Organic light-emitting devices (OLEDs) are currently attracting attention because of the increasing interest in their potential applications as full-color flat-panel displays, lighting sources, and flexible displays [1–4]. The promising applications of OLEDs have led to considerable efforts to fabricate OLEDs with high efficiency and low power consumption [5,6]. Various techniques for developing phosphorescent materials, various structure designs for enhancing exciton confinement in the emitter layer, and uniquely developed p-i-n and tandem structures have been introduced to enhance the device performance of OLEDs [7–11]. Among the several kinds of techniques for enhancing the efficiency of OLEDs, thermally activated delayed fluorescence (TADF) has been especially attractive due to the ability to harvest triplet excitons [12]. The ability of TADF to harvest triplet excitons is attributed to the reverse intersystem crossing (RISC) process from the triplet excited state ( $T_1$ ) to the singlet excited state ( $S_1$ ) with the assistance of thermal energy, which might result in an internal quantum efficiency of 100% [13]. The energy gap difference between  $S_1$  and  $T_1$  ( $\Delta E_{ST}$ ) for the formation of efficient TADF should be extremely small to reduce the exchange interaction, which is directly proportional to the overlap between the highest occupied molecular orbital (HOMO) and the lowest unoccupied molecular orbital (LUMO) [13]. A small  $\Delta E_{ST}$  might allow intermolecular charge transfer (ICT) between mixed electron-donating molecule (D) and electron-accepting molecule (A) materials [14–17].

Extensive efforts have been made to fabricate exciplex OLEDs based on the TADF concept in order to achieve highly efficient OLEDs [18,19]. Especially, the host exciplex system can be made to exhibit TADF characteristics, bipolar properties and excellent charge balance by moderately adjusting the ratio of D to A. Therefore, an exciplex system should be an excellent host for achieving highly-efficiency fluorescent OLEDs [12,20]. Even though some studies on the efficiency enhancement of exciplex OLEDs have been performed, very

few investigations of the device performances of OLEDs fabricated utilizing blue host exciplex systems have been conducted.

This paper reports highly efficient blue OLEDs based on the blue exciplex host system containing carbazole/thioxanthene-S, S-dioxide (EBCz-ThX) and 2-phenyl-bis-4, 6-(3, 5-di-4-pyridylphenyl)pyrimidine (B4PYPPM). Ultraviolet-visible (UV-vis) spectroscopy and photoluminescence (PL) measurements were conducted to clarify the mechanism behind the exciplex emission. Time-resolved PL measurements were performed to investigate the efficiency of the energy transfer from the exciplex host to the TADF dopant. Current density - voltage - luminance (J-V-L) and electroluminescence (EL) measurements were carried out to investigate the electrical and the optical properties of the OLEDs based on a blue exciplex host system.

## 2. Experimental details

The thickness and the sheet resistivity of the indium-tin-oxide (ITO) thin films deposited on glass substrates were 150 nm and 15 ohm/square, respectively. The ITO-coated glass substrates were cleaned in acetone and methanol by using an ultrasonic cleaner and were then thoroughly rinsed in de-ionized water at 25 °C for 15 min. After the chemically-cleaned ITO-coated glass substrates had been dried by using N<sub>2</sub> gas with a purity of 99.999%, their surfaces were treated with an ultraviolet-ozone gas for 20 min at 25 °C. A poly(3, 4-ethylenedioxythiophene:polystyrene sulfonate (PEDOT:PSS) layer was deposited onto an ITO-coated glass substrate by using a spin-coating method at 5000 rpm for 41 s, after which annealing was done at 130 °C for 30 min in a glove box. After the samples had been transferred into an evaporation chamber, the organic layers and the electrodes were deposited at a substrate temperature of 25 °C and a system pressure of  $1.2 \times 10^{-6}$  Torr. The deposition rates of the organic layers and the metal layer were approximately 1.0 and 2.0 Å/s, respectively. Figure 1 shows schematic energy diagrams of OLEDs (a) without and (b) with an exciplex layer. The structures of the OLEDs consisted of the following layers from the bottom:

**Device A (reference):** ITO/ PEDOT:PSS hole injection layer (HIL)/EBCz-Thx: 1,2-bis(carbazol-9-yl)-4,5-dicyanobenzene (2CzPN) 8 wt% (30 nm) as an electron emitting layer (EML)/B4PYPPM (30 nm) as an electron transport layer (ETL)/LiF (1 nm)/Al cathode (100 nm), as shown in Fig. 1(a).

**Devices B, C, D, and E (exciplex):** ITO/PEDOT:PSS hole injection layer (HIL)/exciplex host:2CzPN (B: 4 wt%, C: 6 wt%, D: 8 wt%, E: 10 wt%) (30 nm) as an EML/B4PYPPM (30 nm) as an ETL/LiF (1 nm)/Al cathode (100 nm), as shown in Fig. 1(b).

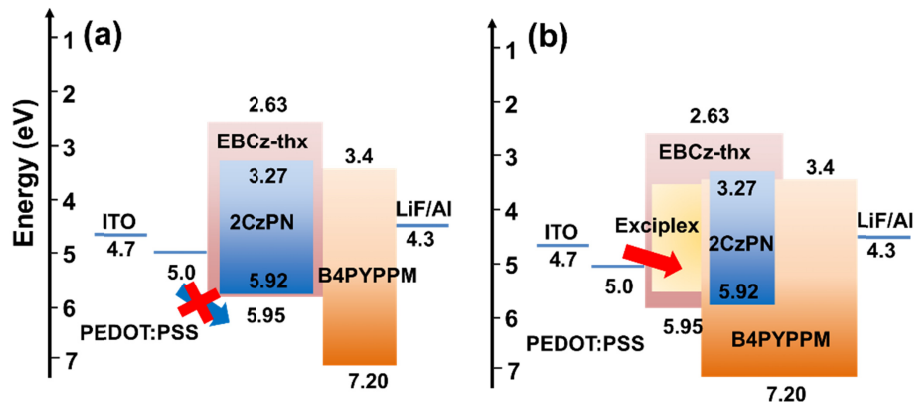


Fig. 1. Schematic energy diagrams of OLEDs (a) without and (b) with an exciplex host layer.

UV-vis absorption spectra were recorded on a spectrophotometer (Shimadzu UV-2500 UV/vis). The PL spectra were measured by using a Perkin-Elmer LS55 fluorescence spectrometer. The time-resolved PL measurements were performed by using an X-ray fluorescence spectrometer (TCSPCFL920) equipped with a pulsed laser operating at a wavelength of 375 nm. J-V-L and EL characteristics were measured by using a Keithley 2400 programmable source meter with built-in current and voltage measurement units (M6100, McScience) and a Minolta CS100 camera. The external quantum efficiency (EQE), current efficiency and power efficiency of the OLEDs were determined from the Lambertian distribution.

### 3. Results and discussion

Figure 2 shows the exciplex emission mechanisms from the exciplex host to the TADF dopant used in this work. The EBCz-Thx has been demonstrated to be an appropriate candidate for efficient exciplex formation due to its consisting of bipolar host materials with wide band-gaps and high  $T_1$  energies [21]. The dynamical process of the excited states for the OLEDs can be explained as follows: Firstly, the exciplex state is formed due to the ICT interaction between EBCz-ThX and B4PYPPM. Excitons are dominantly formed in the exciplex host. Then, because the Förster energy transfer process from the exciplex host to 2CzPN generates singlet excitons in 2CzPN, fluorescence resulting from the decay of the singlet excitons in 2CzPN is emitted. The triplet excitons generated under electrical excitation or derived from the intersystem crossing process can be thermally converted into delayed singlet excitons via the RISC process, resulting in the formation of delayed singlet excitons in 2CzPN due to the Förster energy transfer process from the exciplex host to 2CzPN. Finally, the partial triplet excitons are transferred from the exciplex host to 2CzPN through the Dexter energy transfer process. These triplet excitons can be thermally converted into singlet excitons due to the RISC process resulting from the delayed fluorescence emitted from 2CzPN. Therefore, all excitons from the host and the dopant can contribute to the emission from the OLEDs.

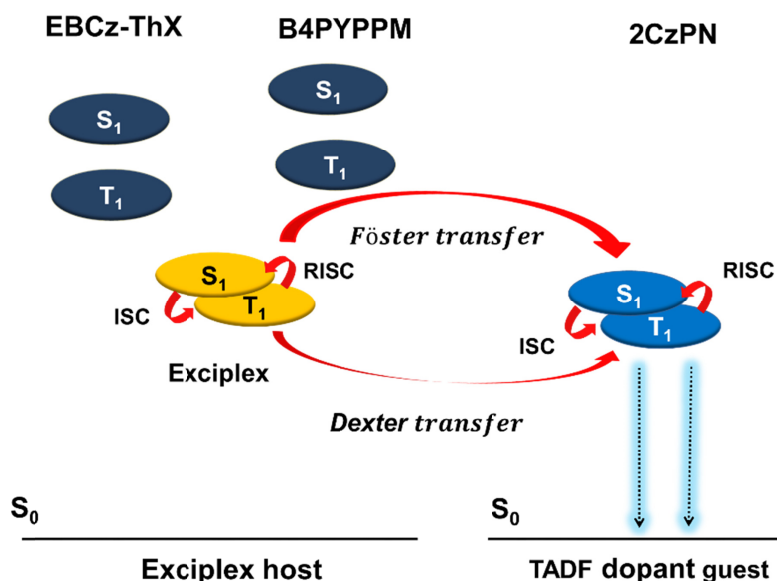


Fig. 2. Schematic diagram of the exciplex emission mechanism from the exciplex host to the TADF dopant.

Figure 3(a) shows the normalized absorption and PL spectra of the EBCz-ThX, the B4PYPPM, and the EBCz-ThX:B4PYPPM (1:1) films. While the absorption peaks at 218, 235, and 274 nm for the EBCz-ThX:B4PYPPM film correspond to the overlapped peaks of the EBCz-ThX film, the intensities of the absorption peaks corresponding to the peaks of the B4PYPPM film are increased in comparison with those of the EBCz-ThX film, indicative of a decrease in the charge interaction for the ground state of the mixed film. Therefore, the CT complex of the ground state does not appear for the EBCz-ThX:B4PYPPM film [22]. The dominant PL peaks for the EBCz-ThX, the B4PYPPM, and the EBCz-ThX:B4PYPPM films appear at 415, 379, and 442 nm, respectively. The main PL peak of the EBCz-ThX:B4PYPPM mixed film is significantly red-shifted in comparison with those of the EBCz-ThX and the B4PYPPM films. The exciplex emission peak of the EBCz-ThX:B4PYPPM film at 2.81 eV is close to the offset value between the LUMO of B4PYPPM (3.4 eV) and the HOMO of EBCz-ThX (5.95 eV). The exciplex state of the EBCz-ThX:B4PYPPM film is ultimately formed due to the existence of the ICT system. Figure 3(b) shows the PL characteristics at 325 nm at low (77 K) and room (300 K) temperatures for the EBCz-ThX:B4PYPPM film. The  $\Delta E_{ST}$  of the EBCz-ThX:B4PYPPM film is 0.03 eV, which is the difference between the  $S_1$  and the  $T_1$  levels of 3.162 and 3.159 eV, respectively, as measured from the room- and the low-temperature PL spectra. Because  $\Delta E_{ST}$  is small enough, the RISC process from the  $T_1$  to the  $S_1$  states can occur with the assistance of thermal energy. The molecular structures of EBCz-Thz and B4PYPPM are schematically shown in Fig. 3(c). The ICT interaction is dominantly generated because of the strong electron-donating property of the ethyl-carbazole in EBCz-ThX and the strong electron-accepting property of the pyridine or the pyrimidine in B4PYPPM. A small  $\Delta E_{ST}$  can be achieved due to the ICT interaction, resulting in the occurrence of exciplex emission.

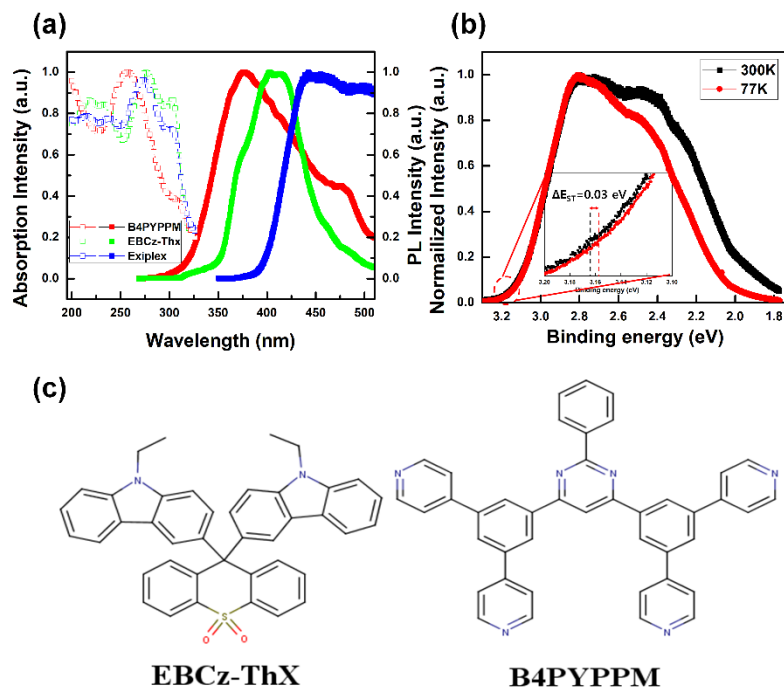


Fig. 3. (a) Normalized absorption and photoluminescence spectra of the B4PYPPM, the EBCz-ThX, and the EBCz-ThX:B4PYPPM (exciplex) films, (b) low and room temperature photoluminescence spectra of the exciplex film, and (c) schematic diagrams of the molecular structures of EBCz-Thz and B4PYPPM.

Figure 4 shows the time-resolved PL characteristics at 375 nm for the EBCz-ThX:B4PYPPM:2CzPN and the EBCz-ThX:2CzPN films. The decays of the PL as functions of time for the EBCz-ThX:B4PYPPM:2CzPN and the EBCz-ThX:2CzPN films can be expressed as double-exponential functions:

$$f(t) = A + B_1 \exp(-t/\tau_1) + B_2 \exp(-t/\tau_2), \quad (1)$$

where  $A$  is the absorption value at 375 nm,  $B_1$  and  $B_2$  correspond to coefficients,  $t$  is the measurement time, and  $\tau_1$  and  $\tau_2$  are the values of the exciton lifetimes. The decays of the PL as functions of time exhibit two lifetimes. While the long and the short exciton lifetimes for the EBCz-ThX:2CzPN film are 3.67 and 1.16  $\mu\text{s}$ , respectively, those of the EBCz-ThX:B4PYPPM:2CzPN film are 4.38 and 1.52  $\mu\text{s}$ . The amplitude-weighted average exciton lifetime is given by,

$$\tau_{\text{avg}} = \sum \tau_k f_k, \quad f_k = B_k / \sum B_i, \quad (2)$$

where  $\tau_k$  and  $f_k$  are the exciton lifetime and the fractional intensity, respectively. The values of  $\tau_{\text{avg}}$  for the decays of the PL decay as functions of time for the EBCz-ThX:2CzPN and the EBCz-ThX:B4PYPPM:2CzPN films are 2.18 and 2.24  $\mu\text{s}$ , respectively. The fitting parameters for PL decay spectra of the EBCz-ThX:2CzPN and the EBCz-ThX:B4PYPPM:2CzPN films are summarized in Table 1. The PL decay time is related to the efficiency of the energy transfer from the exciplex host to the dopant. The PL decay time of the EBCz-ThX:B4PYPPM:2CzPN film is longer than that of the EBCz-ThX:2CzPN film due to the delayed emission of the PL. The energy of the delayed singlet excitons derived from the RISC process of the EBCz-ThX:2CzPN film transfers to the singlet state of 2CzPN via the Förster energy transfer process, resulting in delayed PL emission.

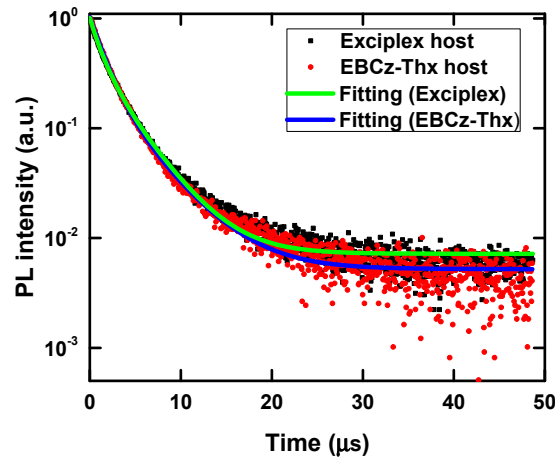


Fig. 4. Time-resolved photoluminescence spectra of the EBCz-ThX:B4PYPPM:2CzPN and the EBCz-ThX:2CzPN films at 375 nm.

**Table 1. Fitting parameters for the PL decay spectra of the EBCz-ThX:2CzPN and the EBCz-ThX:B4PYPPM:2CzPN films.**

Parameters	$\tau_1$	$\tau_2$	B1	B2	A
EBCz-ThX:2CzPN	1.16E-6s	3.66E-6s	0.6231	0.4290	0.00718
EBCz-ThX: B4PYPPM:2CzPN	1.52E-6s	4.38E-6s	0.7752	0.2590	0.00521

Figure 5 shows the (a) current density - voltage (J-V) and the current efficiency - power efficiency - current density for OLEDs with a blue exciplex host. The J-V characteristics of devices A, B, C, D, and E are shown in Fig. 5(a). The operating voltage of devices A, B, C, D, and E at  $10 \text{ mA/cm}^2$  were 14.75, 12.55, 11.82, 10.16, and 13.58 V, respectively. The operating voltage of device A was larger than those of the other devices due to the large energy barrier between the PEDOT:PSS and the EBCz-ThX layers. While electrons transfer from the Al electrode to the EML, holes move from the ITO electrode to the EML. However, the large energy barrier of 0.95 eV between the PEDOT:PSS and the EBCz-ThX layers interrupts the efficient flow of holes, resulting from a decrease in the current density. The current densities of devices B, C, D, and E are larger than that of device A due to the existence in the exciplex energy band of a mixed layer of EBCz-ThX and B4PYPPM. The holes easily move from the PEDOT:PSS layer to the exciplex region, resulting in an increase in the current density. The operating voltage of device D is 4.59 V lower than that of device A due to an increase in the number of injected holes. Figure 5(b) shows the current and the power efficiencies of devices A, B, C, D, and E. The maximum current efficiency and power efficiency of the optimized exciplex OLED (device D) were 22.46 cd/A and 28.23 lm/W, respectively. The current and the power efficiencies of device D were 2 cd/A and 11.62 lm/W higher than those of device A (20.46 cd/A, 16.61 lm/W). The enhanced efficiency of device D is attributed to an increase in the hole injection efficiency and to the enhanced Förster energy transferred from the exciplex host to 2CzPN due to the formation of delayed singlet excitons in the exciplex host. The enhancement of the current and the power efficiencies for device D is related to the increased hole injection efficiency and the TADF property of the exciplex host. The increase in the efficiency roll off for device E might be caused by the exciton annihilation process [23].

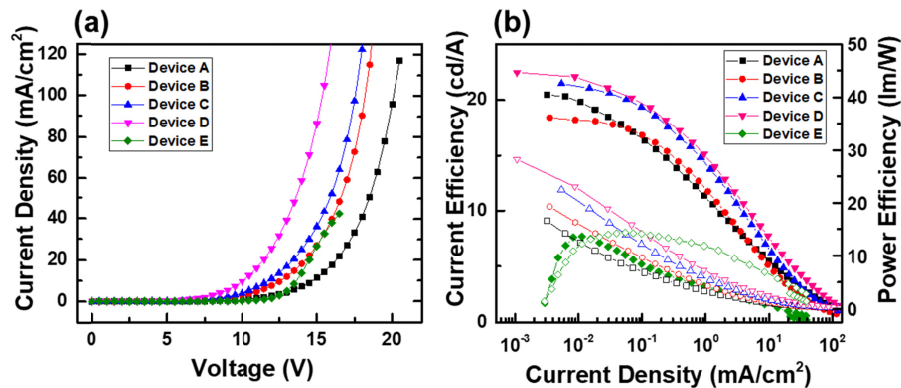


Fig. 5. (a) Current density - voltage and (b) current - power efficiencies - voltage characteristics for OLEDs with an exciplex host.

Figure 6(a) shows the EL spectra of devices A, B, C, D, and E at  $100 \text{ cd/m}^2$ . The peaks of EL spectra for the OLEDs are blue-shifted and the exciplex emission intensity gradually decreases and eventually disappears with increasing 2CzPN concentration. The shape of the EL spectra becomes similar to that for the emission from device A with increasing 2CzPN concentration. The disappearance of the exciplex emission is related to the energy transfer from the exciplex host to 2CzPN. While the position of the EL peak for device D (490 nm) is almost the same as that for device A (494 nm), the EL peaks for devices B and C are red-shifted in comparison with that for device A. The variation in the emission wavelength is attributed to incomplete energy transfer from the exciplex to the fluorescent dopant, and the single emission peak is related to the overlapping of the emission bands of the exciplex and the dopant.

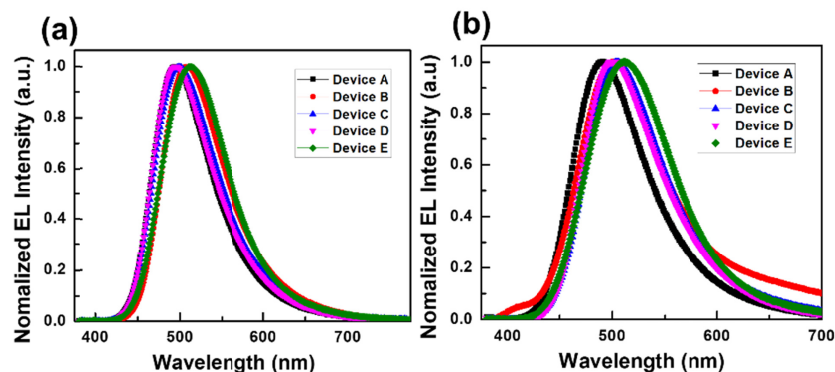


Fig. 6. Electroluminescence spectra for OLEDs with a blue exciplex host at (a) 100 and (b) 1000  $\text{cd/m}^2$ .

However, the EL spectra for the OLEDs show only a single emission peak, which corresponds to the emission from 2CzPN [24]. While the exciplex peak for device B begins to appear with increasing luminance to 1000  $\text{cd/m}^2$ , the dominant peak of 2CzPN still exists and does not shift, as shown in Fig. 6(b). This behavior is attributed to a shift in the wavelength of the emission resulting from an overlap of the exciplex and the 2CzPN emissions. The shift of the 2CzPN peak originates from either molecular polarization effects [25,26] or a variation in the dielectric constant of the EML [25]. The peak of the EL spectrum for device E shifts to the red emission region in comparison with that for the other devices due to the exciton quenching process resulting from increases in the numbers of the excitons in the exciplex host.

#### 4. Summary and conclusions

OLEDs were fabricated with a blue EBCz-ThX:B4PYPPM exciplex host system in order to enhance their efficiency. UV-vis and PL spectra showed exciplex emission resulting from the ICT interaction between the ethyl-carbazole in EBCz-ThX and the pyridine in B4PYPPM. The maximum values of the current and the power efficiency of the OLEDs with a blue exciplex host were 22.46  $\text{cd/A}$  and 28.23  $\text{lm/W}$ , respectively. The efficiency enhancement for the OLEDs based on an exciplex system acting as a TADF emitter was attributed to the efficient up-conversion of triplet excitons in EBCz-thx:B4PYPPM and to the efficient energy transfer from the exciplex host to the blue TADF emitter. These present observations can help to improve our understanding of the EBCz-ThX:B4PYPPM exciplex host system and its ability to enhance the efficiency of OLEDs.

#### Funding

Basic Science Research Program through the National Research Foundation of Korea (NRF) funded by the Ministry of Education, Science and Technology (2016R1A2A1A05005502).

#### Acknowledgments

The authors sincerely thank Dr. I. K. Moon for supplying the EBCz-ThX material.

#### References

1. N. S. Höfle, M. Pfaff, H. Do, C. Bernhard, D. Gerthsen, U. Lemmer, and A. Colmann, "Suppressing molecular aggregation in solution processed small molecule organic light emitting diodes," *Org. Electron.* **15**(1), 337–341 (2014).
2. D. H. Kim and T. W. Kim, "Efficiency enhancement of organic light-emitting devices due to a localized surface plasmonic resonance effect of poly(4-butylphenyl-diphenyl-amine):dodecanethiol functionalized Au nanocomposites," *Opt. Express* **23**(9), 11211–11220 (2015).

3. Z. Wang, X. -L. Li, Z. Ma, X. Cai, C. Cai, and S. -J. Su, "Exciton-adjustable interlayers for high efficiency, low efficiency roll-off, and lifetime improved warm white organic light-emitting diodes (WOLEDs) based on a delayed fluorescence assistant host," *Adv. Funct. Mater.* **28**(11), 1706922 (2018).
4. H. J. Shin and T. W. Kim, "Ultra-high-image-density large-size organic light-emitting devices based on In-Ga-Zn-O thin-film transistors with a coplanar structure," *Opt. Express* **26**(13), 16805–16812 (2018).
5. D. H. Kim and T. W. Kim, "Efficiency enhancement in tandem organic light-emitting devices with a hybrid charge generation layer composed of BEDT-TTF-doped TPBi/mCP/HAT-CN," *Org. Electron.* **15**(12), 3452–3457 (2014).
6. D. H. Kim and T. W. Kim, "Highly efficient organic light-emitting devices based on poly(N,N'-bis-4-butylphenyl-N,N'-bisphenyl)benzidine:octadecylamine-graphene quantum dots," *Org. Electron.* **57**, 305–310 (2018).
7. C. W. Tang, S. A. Van Slyke, and C. H. Chen, "Electroluminescence of doped organic thin films," *Appl. Phys. Lett.* **65**(9), 3610–3616 (1989).
8. M. A. Baldo, D. F. O'Brien, Y. You, A. Shoustikov, S. Sibley, M. E. Thompson, and S. R. Forrest, "Highly efficient phosphorescent emission from organic electroluminescent devices," *Nature* **395**(6698), 151–154 (1998).
9. K. Goushi, R. Kwong, J. J. Brown, H. Sasabe, and C. Adachi, "Triplet exciton confinement and unconfinement by adjacent hole-transport layers," *Appl. Phys. Lett.* **95**(12), 7798–7802 (2004).
10. S. Su, E. Gonmori, H. Sasabe, and J. Kido, "Highly efficient organic blue- and white-light-emitting devices having a carrier- and exciton-confining structure for reduced efficiency roll-off," *Adv. Mater.* **20**(21), 4189–4194 (2008).
11. L. S. Liao, K. P. Klubek, and C. W. Tang, "High-efficiency tandem organic light-emitting diodes," *Appl. Phys. Lett.* **84**(2), 167–169 (2004).
12. J. W. Sun, K.-H. Kim, C.-K. Moon, J.-H. Lee, and J.-J. Kim, "Highly efficient sky-blue fluorescent organic light emitting diode based on mixed cohost system for thermally activated delayed fluorescence emitter (2CzPN)," *ACS Appl. Mater. Interfaces* **8**(15), 9806–9810 (2016).
13. H. Uoyama, K. Goushi, K. Shizu, H. Nomura, and C. Adachi, "Highly efficient organic light-emitting diodes from delayed fluorescence," *Nature* **492**(7428), 234–238 (2012).
14. A. Endo, K. Sato, K. Yoshimura, T. Kai, A. Kawada, H. Miyazaki, and C. Adachi, "Efficient up-conversion of triplet excitons into a singlet state and its application to organic light emitting diodes," *Appl. Phys. Lett.* **98**(8), 083302 (2011).
15. S. Y. Lee, T. Yasuda, H. Nomura, and C. Adachi, "High-efficiency organic light-emitting diodes utilizing thermally activated delayed fluorescence from triazine-based donor–acceptor hybrid molecules," *Appl. Phys. Lett.* **101**(9), 093306 (2012).
16. K. Goushi, K. Yoshida, K. Sato, and C. Adachi, "Organic light-emitting diodes employing efficient reverse intersystem crossing for triplet-to-singlet state conversion," *Nat. Photonics* **6**(4), 253–258 (2012).
17. K. Goushi and C. Adachi, "Efficient organic light-emitting diodes through upconversion from triplet to singlet excited states of exciplexes," *Appl. Phys. Lett.* **101**(2), 023306 (2012).
18. H. Shin, S. Lee, K. H. Kim, C. K. Moon, S. J. Yoo, J. H. Lee, and J. J. Kim, "Blue phosphorescent organic light-emitting diodes using an exciplex forming co-host with the external quantum efficiency of theoretical limit," *Adv. Mater.* **26**(27), 4730–4734 (2014).
19. X. K. Liu, Z. Chen, J. Qing, W. J. Zhang, B. Wu, H. L. Tam, F. Zhu, X. H. Zhang, and C. S. Lee, "Remanagement of singlet and triplet excitons in single-emissive-layer hybrid white organic light-emitting devices using thermally activated delayed fluorescent blue exciplex," *Adv. Mater.* **27**(44), 7079–7085 (2015).
20. Y. Seino, S. Inomata, H. Sasabe, Y. J. Pu, and J. Kido, "High-Performance Green OLEDs Using Thermally Activated Delayed Fluorescence with a Power Efficiency of over 100 lm W(-1)," *Adv. Mater.* **28**(13), 2638–2643 (2016).
21. Y. P. Jeon, K. S. Kim, K. K. Lee, I. K. Moon, D. C. Choo, J. Y. Lee, and T. W. Kim, "Blue phosphorescent organic light-emitting devices based on carbazole/thioxanthene-S,S-dioxide with a high glass transition temperature," *J. Mater. Chem. C Mater. Opt. Electron. Devices* **3**(24), 6192–6199 (2015).
22. T. Zhang, B. Zhao, B. Chu, W. Li, Z. Su, L. Wang, J. Wang, F. Jin, X. Yan, Y. Gao, H. Wu, C. Liu, T. Lin, and F. Hou, "Blue exciplex emission and its role as a host of phosphorescent emitter," *Org. Electron.* **24**, 1–6 (2015).
23. M. Mamada, K. Inada, T. Komino, W. J. Potscavage, Jr., H. Nakanotani, and C. Adachi, "Highly efficient thermally activated delayed fluorescence from an excited-state intramolecular proton transfer system," *ACS Cent. Sci.* **3**(7), 769–777 (2017).
24. D. Y. Zhou, H. Z. Siboni, Q. Wang, S. S. Liao, and H. Aziz, "Host to guest energy transfer mechanism in phosphorescent and fluorescent organic light-emitting devices utilizing exciplex-forming hosts," *J. Phys. Chem. C* **118**(4), 24006–24012 (2014).
25. C. H. Chen, C. W. Tang, J. Shi, and K. P. Klubek, "Improved red dopants for organic electroluminescent devices," *Macromol. Symp.* **125**(1), 49–58 (1998).
26. V. Bulović, A. Shoustikov, M. A. Baldo, E. Bosea, V. G. Kozlova, M. E. Thompson, and S. R. Forrest, "Bright, saturated, red-to-yellow organic light-emitting devices based on polarization-induced spectral shifts," *Chem. Phys. Lett.* **287**(3–4), 455–460 (1998).